



Crop-driven optimization of agrivoltaics using a digital-replica framework

Emre Mengi^{a,*}, Omar A. Samara^b, Tarek I. Zohdi^a

^a Department of Mechanical Engineering, 6102 Etcheverry Hall, University of California, Berkeley, 94720-1740, CA, USA

^b Department of Biological and Agricultural Engineering, 1 Shields Ave., University of California, Davis, 95616-5270, CA, USA

ARTICLE INFO

Editor: Spyros Fountas

Keywords:

Agrivoltaics
Simulation
Crop modeling
Genomic optimization

ABSTRACT

Agrivoltaics are a novel form of agricultural production where photovoltaic panels are blended with crops in order to optimize land use, particularly with respect to crop production and power generation. Given agrivoltaics are complicated systems where crop production, water use efficiency, land use efficiency, solar energy production, and the economics of the entire system are all dependent and competing for solar energy, there is opportunity to develop models incorporating these objectives into an optimizable framework. This work contributes to agrivoltaic design methodology through a digital replica and genomic optimization framework which simulates light rays in a procedurally generated agrivoltaic system at an hourly timestep for a defined crop, location and growing season to model light absorption by the photovoltaic panels and the crop below. Hourly radiation values are then summed into daily radiation values and fed into a crop model to simulate performance of an agrivoltaic and a reference crop at a daily timestep. The results of photovoltaic and crop performance metrics for a given design are then used in a genomic optimization algorithm to conduct a multi-objective optimization across various designs to find an optimal, crop-driven solution for a defined crop, season and location. A numerical example is demonstrated using this framework with a SunnySD tomato crop grown in Davis, California, resulting in 28.9% optimization of combined crop and energy production using a genomic optimization scheme over 50 generations.

1. Introduction

Agrivoltaic technology is a rapidly evolving field which has seen increasing activities since 2011 with a series of well cited studies occurring in Montpellier, France [1–4]. The scale and scope of agrivoltaic experiments range from simulations and mathematical models, to field experiments [5,6]. Additionally, agrivoltaics include a wide range of systems which fall largely into the category of greenhouses [7,8] and photovoltaic arrays in fields [9,10] which will be the subject of this model. Photovoltaic arrays in agricultural fields, considered field style agrivoltaics, are a form of agrivoltaics where photovoltaic arrays are placed over agricultural crops (Fig. 1) to manage energy balance into the system. There are many reasons to use agrivoltaic systems, including improved land use efficiency, economic value of electricity, optimized crop microclimate and reduced water use, but ultimately all of them require a framework for evaluation of their performance in order to design and optimize a given design.

A number of modeling frameworks have been presented which approach agrivoltaic modeling combining the light simulation of photovoltaics and the dynamics of how photovoltaics will impact the agricultural component of the related crop response [9,11,12]. Efforts have also been made to optimize agrivoltaic designs [13,14], but given the complexity and various potential optimization parameters (photosynthetic performance, energy production, land use efficiency, economic performance, etc.) there is still opportunity to develop optimization schemes which focus on different aspects of agrivoltaic performance. This work proposes contributing to agrivoltaic design methodology by utilizing a digital replica framework centered around crop production which first simulates light into an agrivoltaic system to model photovoltaic and crop performance and using the outputs of these models in conjunction with a multi-objective genomic optimization algorithm to rapidly evaluate agrivoltaic design performance across various metrics (energy and crop production, light and water use efficiency) and find a crop centered solution for a given crop and place.

* Corresponding author.

E-mail address: emre_mengi@berkeley.edu (E. Mengi).



Fig. 1. Field style agrivoltaic system designed in Unity3D.

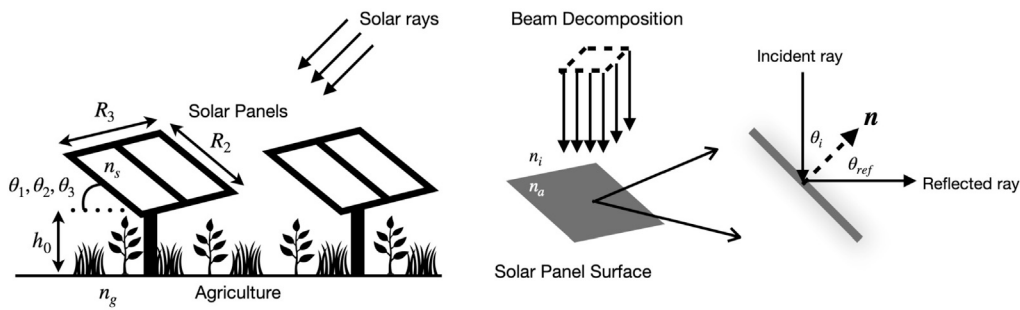


Fig. 2. Left: Modeled APV system. Right: Beam decomposition for the raytracing model.

2. Digital replica model

A digital replica model is a simulation framework where a replica of a physical system can be used for analysis, optimization, and manipulation without the real-world cost of building the physical system. A digital-replica of an agrivoltaic system can be created to run physics simulations to assess agrivoltaic performance. This method has been previously explored by the authors and the reader is referred to Zohdi [15] and Isied et al. [16] for details on creating such a framework. The said framework was built to assess the agrivoltaic performance in terms of ground and solar panel absorption of light using a geometric raytracing method. This study aims to combine the raytracing framework with a crop model to evaluate agrivoltaic performance based on a crop-centered approach. A digital replica of an open-field agrivoltaic system is generated using the light model and the crop model to optimize the system design over a specified crop-season with associated ambient parameters.

2.1. Light model

2.1.1. Model assumptions

The light model simulates a light-pulse applied to the agrivoltaic system at hourly time intervals for hours where the sun is above horizon for every day in a specified crop season. Solar angles are simulated using an open-source python package, called `pysolar` [17], while solar radiation values are read from a weather file. Increasing the number of simulated days rapidly increase run time for the simulation, therefore, certain assumptions are made to reduce computational load:

- The solar panels are identical in shape, installation angle, and material,
- The light model flashes a unit area of the agrivoltaic field, assuming the distribution of solar panels on the field is uniform,

- The solar panels are bifacial, therefore able to absorb energy reflected from ground and other solar panels.

The detailed assumptions regarding the raytracing framework can be found in Zohdi [15].

2.1.2. Solar panel geometry

The solar panel geometry is assumed to be known and described by a surface function, $F(x_1, x_2, x_3)$. The solar panels shapes are generated using the 3D-ellipsoidal equation:

$$F(x_1, x_2, x_3) = \left| \frac{x_1 - x_{1o}}{R_1} \right|^{p_1} + \left| \frac{x_2 - x_{2o}}{R_2} \right|^{p_2} + \left| \frac{x_3 - x_{3o}}{R_3} \right|^{p_3} \quad (1)$$

where (R_1, R_2, R_3) are the generalized radii, (p_1, p_2, p_3) are the exponents of the generalized ellipsoid, and (x_{1o}, x_{2o}, x_{3o}) are the center location of the ellipsoid. These are the design parameters we will optimize using the genomic optimization framework. Fig. 3 shows various shapes the solar panels can attain.

Rays traveling through the system collide with the solar panels if $F(x_{1,j}, x_{2,j}, x_{3,j}) \leq 1$, where j indicates each ray. As the agrivoltaic system includes more than one panel on the field, the algorithm will check if a ray has collided with any of the solar panels located at $(x_{1o,i}, x_{2o,i}, x_{3o,i})$. Similarly, the ray is assumed to hit the ground surface if $x_{3,j} \leq 0$. The power absorption by the surface and power reflected by the ray can be determined using reflectivity calculations, which are described in the next section.

2.1.3. Raytracing algorithm

It is assumed the light incident on the agrivoltaic system can be discretized as a collection of rays, which are propagated through the system using a time-stepping scheme. The initial collective power of the rays, P_{tot} , is read from a weather file for the given date, time, and location as the clear sky radiation given in $\frac{W}{m^2}$. A square beam is initial-

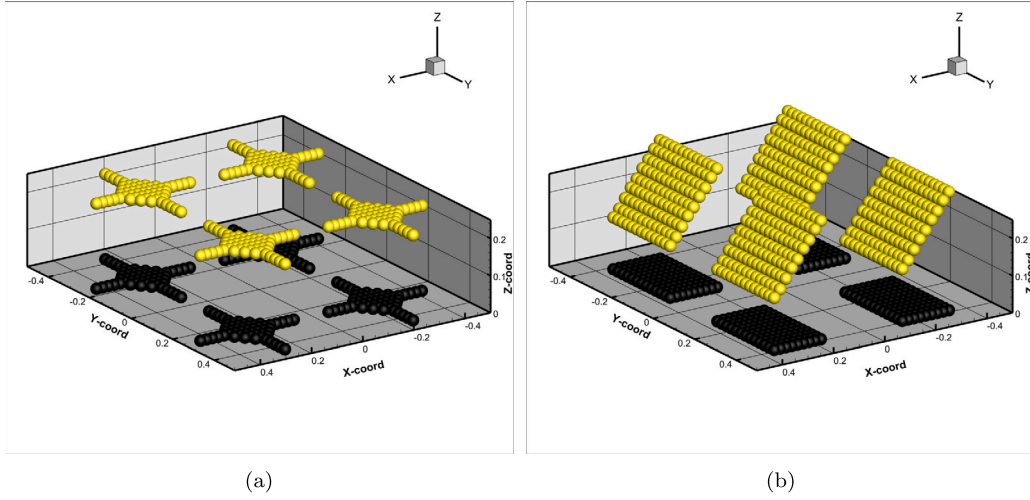


Fig. 3. Example solar panel shapes generated using the 3D-ellipsoidal equation for (a) $(\theta_1, \theta_2, \theta_3) = (0, \pi/2, \pi/2)$, $(R_1, R_2, R_3) = (0.002, 0.2, 0.2)$, $(p_1, p_2, p_3) = (5, 1/2, 1/2)$ and (b) $(\theta_1, \theta_2, \theta_3) = (0, -\pi/4, 0)$, $(R_1, R_2, R_3) = (0.002, 0.15, 0.15)$, $(p_1, p_2, p_3) = (20, 20, 20)$. The shadow cast by the panels at noon can be seen on the ground surface.

ized at the appropriate position and velocity in order to hit the entirety of the field at any given sun angle. Initial power of an individual ray is defined as:

$$P_r = \frac{P_{tot} A_b}{N_r} \quad (2)$$

where A_b is the area of the square beam and N_r is the number of rays used in the discretization of the sunlight beam. When a ray hits a surface (Fig. 2), the inward surface normal is calculated at the point the ray has intersected the surface:

$$\mathbf{n} = -\frac{\nabla F}{\|\nabla F\|} \quad (3)$$

where ∇F is the gradient of the solar panel. For the ground surface, the surface is assumed to be flat and has the normal $\mathbf{n} = [0, 0, -1]$. Using the surface normal and the incoming ray velocity vector, the angle of incidence (θ_i) can be calculated as

$$\theta_i = \cos^{-1} \left(\frac{\mathbf{v}_j \cdot \mathbf{n}_j}{\|\mathbf{v}_j\| \|\mathbf{n}_j\|} \right) \quad (4)$$

The ray velocity perpendicular to the surface normal can be calculated as

$$\mathbf{v}_{j,\perp} = \|\mathbf{v}_j\| \cos \theta_i \mathbf{n}_j \quad (5)$$

The reflected ray velocity is then calculated (\mathbf{v}_j^{ref}) by subtracting the perpendicular velocity component twice from the initial ray velocity:

$$\mathbf{v}_j^{ref} = \mathbf{v}_j - 2\mathbf{v}_{j,\perp} \quad (6)$$

Finally, power absorbed by the surface is calculated and retained by the ray using the reflectance parameter, \mathcal{R} . The ratio of the amount of reflected electromagnetic energy per unit time (I_r) to the incident electromagnetic energy per unit time (I_i) is assumed to be given by total reflectance $\mathcal{R} \equiv \frac{I_r}{I_i}$ where $0 \leq \mathcal{R} \leq 1$ for unpolarized electromagnetic radiation. The reflectance is dependent on the angle of incidence and the refractive index ratio (\hat{n}) of the solar panels to the ambient medium, which is assumed to be a vacuum for the purposes of raytracing. The refractive index ratio is calculated as

$$\hat{n} = \frac{n_a}{n_i} \quad (7)$$

The absorbing medium refractive index, n_a , is part of the design space and is determined by the genomic optimization framework. The incident refractive index is assumed to be $n_i = 1$ (vacuum). The reflectivity \mathcal{R} can be calculated as

$$\mathcal{R}(\hat{n}, \theta_i) = \frac{I_r}{I_i} \quad (8)$$

$$= \frac{1}{2} \left(\frac{\hat{n}^2 \cos \theta_i - (\hat{n}^2 - \sin^2 \theta_i)^{\frac{1}{2}}}{\hat{n}^2 \cos \theta_i + (\hat{n}^2 - \sin^2 \theta_i)^{\frac{1}{2}}} \right)^2 + \left(\frac{\cos \theta_i - (\hat{n}^2 - \sin^2 \theta_i)^{\frac{1}{2}}}{\cos \theta_i + (\hat{n}^2 - \sin^2 \theta_i)^{\frac{1}{2}}} \right)^2 \quad (9)$$

The details of the derivation of \mathcal{R} is given in Zohdi [15]. The surface power absorption and ray power retention are calculated at each ray-surface interaction throughout the simulation. The power absorbed by the surface can be calculated by

$$P_{abs} = (1 - \mathcal{R})P_r \quad (10)$$

The remaining power in the ray is calculated as follows:

$$P_{ref} = \mathcal{R}P_r \quad (11)$$

The ray is tracked in the system as long as:

- the ray is within the system domain limits,
- its power is above the specified power threshold P_{min} .

The rays are propagated in the system using explicit Forward Euler time-stepping scheme. The raytracing algorithm can be described by the following steps:

1. Initialize ray positions $\mathbf{r}_j(t=0)$ and velocities $\mathbf{v}_j(t=0)$.
2. Check for surface-ray collisions. IF a ray intersects a surface:
 - (a) Update power absorbed by the surface and remaining power of the ray,
 - (b) Calculate the reflected ray velocity.
3. Check for active rays:
 - (a) End simulation IF all rays are deactivated,
 - (b) Continue to next step IF any of the rays are active.
4. Iterate ray positions in time using:

$$\mathbf{r}_j(t + \Delta t) = \mathbf{r}_j(t) + \Delta t \mathbf{v}_j(t) \quad (12)$$

5. Increment the time step to $(t = t + \Delta t)$ and go back to Step 2.

The time-step size Δt is chosen using the formula $\Delta t = \xi \frac{h_0^{ray}}{c}$, where h_0^{ray} is the initial height of the generated rays, c is the speed of light, and ξ is a tunable parameter such that $\xi \in (0, 1]$. The speed of the light requires a time step size scaled to accurately observe the motion of the rays with a sufficient number of time steps. For this work, the parameter is chosen to be $\xi = 0.01$

2.2. Crop model

Crop modeling aims to take in measured inputs and an understanding of plant physiological processes to determine when and how a crop will grow. This framework utilizes the SIMPLE Crop Model [18].

2.2.1. SIMPLE crop model

The SIMPLE Crop Model is a model designed to simplify crop modeling to basic components. It is well validated and uses simple parameters allowing for straightforward and fast implementation. The model works on a daily time step by first looking at the crop's temperature, and determining where in the growth process it should be through cumulative thermal time. Once crop temperature is determined to be within the proper range, the growth stage and light input plus other crop parameters are used to simulate daily biomass growth, which is then summed through the season. At the end of the season, the cumulative biomass is multiplied by a harvest index to represent yield. The exact details are delineated in the original publication [18], but are summarized below:

$$B_{rate} = P \times f(\text{Solar}) \times RUE \times f(\text{CO}_2) \times f(\text{Temp}) \times \min(f(\text{Heat}), f(\text{Water})) \quad (13)$$

$$B_{cumulative,i+1} = B_{cumulative,i} + B_{rate} \quad (14)$$

$$\text{Yield} = B_{cumulative,maturity} \times HI \quad (15)$$

Where B_{rate} and $B_{cumulative}$ is the daily biomass gain and cumulative biomass respectively, HI is the crop specific harvest index, and P is the daily radiation into the system.

Agrivoltaic theory is built on the analysis of CO_2 limited photosynthesis at high light levels resulting in a light saturation point [19–22] which facilitates dual use of the energy in excess to crop demands. While it would be preferable to use a more representative photosynthesis model to simulate plant growth, this paper presents an agrivoltaic modeling framework and any crop model will serve as a substitute. It is not strictly necessary to undergo the complex studies required for a more accurate photosynthesis model to modify the SIMPLE model given the scope of this framework.

The SIMPLE Crop Model also has a robust air temperature response model, but no extensions are included in this framework to model the specific temperature impacts of agrivoltaics for either the air or crop temperatures. While the agrivoltaic literature suggests there is some impact relating to air temperature at the plant level in the agrivoltaic installation [6], previous modeling has shown the overall impact of air temperature differences to not have meaningful impact on plant growth [3] (it is suggested light is the primary driver in any growth differences), particularly if the photovoltaics are sufficiently far from the plants [23] (over 1.5 m). This suggests modeling air temperature dynamics would have marginal impact to this framework while dramatically increasing computational demands and simulation time, and for this reason is not conducted in this framework.

In addition to the outputs of the model, two additional metrics are added: Light Use Efficiency (LUE) and Water Use Efficiency (WUE).

$$LUE = \frac{\text{Yield}}{TLI} \quad (16)$$

$$WUE = \frac{\text{Yield}}{TWD} \quad (17)$$

Where Yield is the total crop yield for the simulated season (which in this case is the system for either the agrivoltaic or the reference crop, depending on which step of the simulation is being done), TLI is the sum total light into the system for the simulated season, and TWD is the sum total reference evapotranspiration for the simulated season as described below:

$$\int_{\text{Planting}}^{\text{Harvest}} P_{crop,daily} dt \quad (18)$$

$$\int_{\text{Planting}}^{\text{Harvest}} ET_o dt \quad (19)$$

The purpose of these additional metrics is to facilitate agriculturally focused optimization which allows for improved agricultural performance without strictly requiring increased yields. To support the WUE calculation, water use was also simulated by utilizing the Penman-Monteith equation to calculate daily reference evapotranspiration (ET_o) as described in [24]. ET_o is chosen over ET_c because the SIMPLE Crop Model does not contain a simple method for integrating crop coefficients (K_c values), and K_c values for agrivoltaic production are not well developed making direct calculation of ET_c values difficult and beyond the scope of the framework.

2.3. Linking the light and crop model

The framework proposed in this study combines the light simulation model with the crop model in order to optimize the agrivoltaic system using crop performance and solar energy production metrics, as seen in the framework diagram in Fig. 4. First, the light model is run to obtain the solar panel power absorption and ground surface power absorption. Daily radiation values obtained through the light-based simulation are then passed into the crop model which calculates the reference and agrivoltaic crop yield via the SIMPLE model. The crop model then outputs agrivoltaic and reference crop yields as well as other crop performance metrics discussed earlier. The entire framework has been built in Python 3.9 with only `numpy` and `pysolar` external packages. The main program with system parameters, the light model, and the genetic algorithm calls the crop model in a secondary program. The light model simulates the sun's position for the crop season and calculates average ground radiation ($\frac{W}{m^2}$), which is then passed onto the crop model to calculate the crop biomass, evapotranspiration, water, and light use for a given agrivoltaic design. This routine is repeated for each agrivoltaic design in the genetic optimizer in each generation to calculate the design fitness, rank designs, and use evolutionary principles to retain the best performers. Currently, the code uses manually inputted system parameters (i.e. weather data, crop type, solar panel properties, etc.) to optimize the design, although it is possible to develop a GUI for crop growers to use this framework for their own choice of crops, solar panels, and location in future extensions.

3. Genomic optimization framework

3.1. Design parameters

The agrivoltaic system design is defined by the following variables:

$$\Lambda^i \equiv \{\Lambda_1^i, \dots, \Lambda_N^i\} \equiv \{\theta_2, \theta_3, \hat{n}_s, \hat{n}_g, h_0, R_2, R_3, p_1, p_2, p_3\} \quad (20)$$

where \hat{n}_s and \hat{n}_g are the refractive indices of the solar panels and the ground, R_2 and R_3 are generalized radii of the solar panels, θ_2 and θ_3 are the solar panel rotation around e_2 and e_3 axes, p_1 , p_2 , and p_3 are the geometric exponents. The thickness of the solar panel, R_1 , and the rotation around e_1 are kept constant. The rotation of solar panels around all three axes is not practical since the panels only need to adjust for the sun altitude and azimuth angles. While only stationary panels are considered for this study, solar tracking panels can be implemented by having one altitude and azimuth angle pair per day as part of the design variables. The design parameters in Λ^i can be chosen within user-specified bounds.

3.2. Design fitness

The "fitness" or cost associated with a given agrivoltaic system design is determined by a custom cost function. A good agrivoltaic design will appropriately distribute incoming sunlight between the solar panels and the ground. However, the ground energy absorption does not

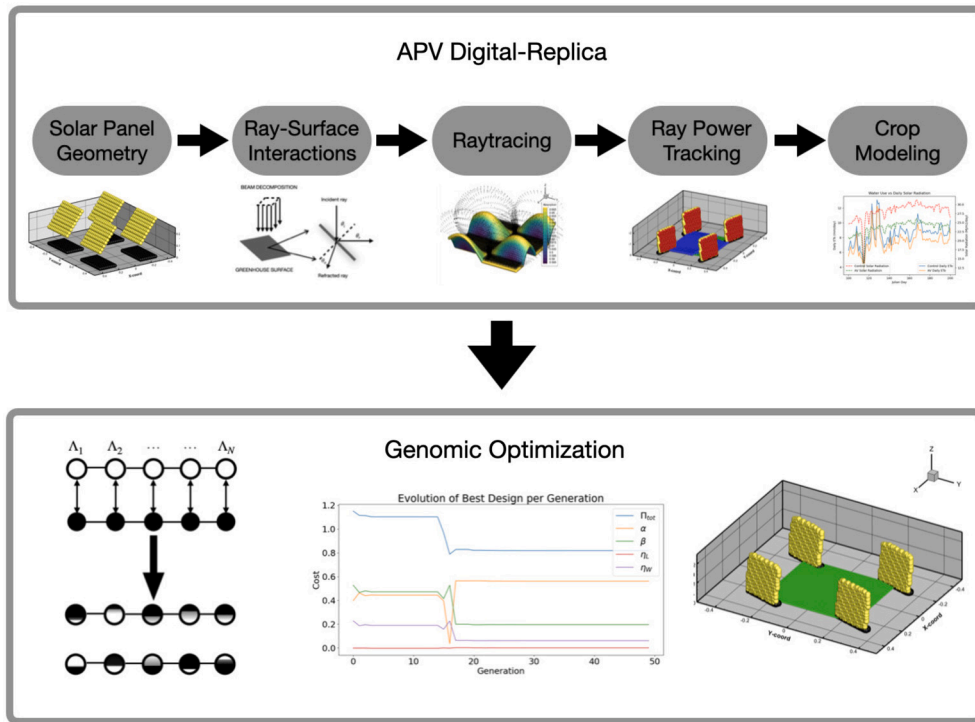


Fig. 4. Digital replica and genomic optimization framework.

fully represent the crop performance. Therefore, the crop yield from the agrivoltaic system needs to be comparable to the reference crop yield, which is independently calculated using the same ambient parameters but without the solar panels on the field. The following cost function is proposed to evaluate the agrivoltaic system performance:

$$\Pi = w_1\alpha + w_2\beta + w_3\eta_L + w_4\eta_W \quad (21)$$

where are defined by the following equations:

$$\alpha = \frac{P_{ref} - P_{solar}}{P_{ref}} \quad (22)$$

$$\beta = \frac{Y_{ref} - Y_{APV}}{Y_{ref}} \quad (23)$$

$$\eta_L = \frac{LUE_{ref} - LUE_{APV}}{LUE_{ref}} \quad (24)$$

$$\eta_W = \frac{WUE_{ref} - WUE_{APV}}{WUE_{ref}} \quad (25)$$

where the weights can be chosen by the user to prioritize the agriculture, solar power generation, etc. The lack of an absolute value function on the agricultural cost parameters enables the optimizer to generate designs that can exceed the reference crop performance in terms of the individual cost parameters, as demonstrated in a 2017 German agrivoltaic potato crop [25] where agrivoltaic yields exceeded the reference yield. While this is a single example, and the SIMPLE crop model cannot strictly replicate this performance, there is the theoretical possibility of a more complicated crop model outputting improved agrivoltaic yields compared to the reference crop. As such, this framework allows for the possibility of improved yields, even if only theoretical, to incentivize high crop yields in the designs. Note that all the cost parameters are non-dimensional and normalized.

3.3. Constraints

There are many critical constraints when considering agrivoltaic design, however, two important ones identified in the literature are considered in this framework:

1. Agrivoltaics should focus on supporting agricultural production and should have a constraint which minimizes the negative impacts of shading on crop yield [26–28],
2. Agrivoltaic land use should not excessively compromise agricultural or photovoltaic production and should have a constraint ensuring the combined land equivalent ratio of agricultural and photovoltaic production is greater than single use of the land for either type of production to ensure any production compromises ultimately yield a net gain to the efficiency of the land use [1,9,29,30].

These two constraints are selected as they well represent the desire for agrivoltaics to provide value centered around agriculture, and can be mathematically described with the following equations:

$$\frac{Y_{APV}}{Y_{ref}} \geq \delta \quad (26)$$

$$\frac{Y_{APV}}{Y_{ref}} + \frac{P_{solar}}{P_{ref}} \geq 1 \quad (27)$$

where Y_{ref} refers to the reference crop yield (no solar panels on field), P_{ref} refers to the reference solar energy generation (no crops) and δ refers to the percent of acceptable loss of crop yield related to installing agrivoltaics. Because these constraints need to be enforced on the cost parameters rather than the design parameters, the design space cannot be limited to acceptable designs *a priori*. One option is to enforce *soft constraints* to the system by including penalty terms in the cost function with very large weights to eliminate designs that do not abide the constraints during the design evaluation process of the genomic optimization framework. The modified cost function can be written as:

$$\Pi = w_1\alpha + w_2\beta + w_3\eta_L + w_4\eta_W + P_1 + P_2 \quad (28)$$

where,

$$P_1 = \begin{cases} 10000 & \text{for } \frac{Y_{APV}}{Y_{ref}} < \delta \\ 0 & \text{for } \frac{Y_{APV}}{Y_{ref}} \geq \delta \end{cases} \quad (29)$$

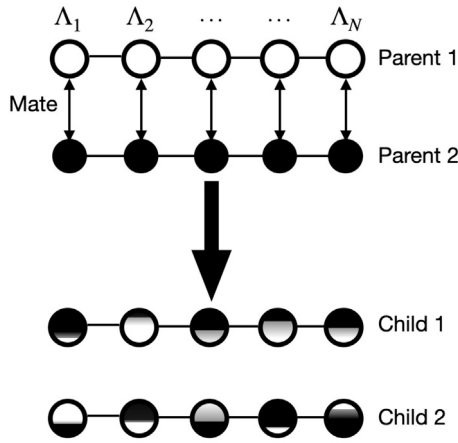


Fig. 5. Children generation from best performing genes (parents).

$$P_2 = \begin{cases} 10000 & \text{for } \frac{Y_{APV}}{Y_{ref}} + \frac{P_{solar}}{P_{ref}} < 1 \\ 0 & \text{for } \frac{Y_{APV}}{Y_{ref}} + \frac{P_{solar}}{P_{ref}} \geq 1 \end{cases} \quad (30)$$

3.4. Genetic algorithm

To apply the genetic algorithm,

1. Generate S random genetic strings, where $\Lambda_i \in [\Lambda_i^-, \Lambda_i^+]$

$$\Lambda = (\Lambda^{(1)}, \Lambda^{(2)}, \dots, \Lambda^{(i)}, \dots, \Lambda^{(S)}) \quad (31)$$

where

$$\Lambda^{(i)} = \begin{pmatrix} \theta_2^- \leq \theta_2^{(i)} \leq \theta_2^+ \\ \dots \\ p_3^- \leq p_3^{(i)} \leq p_3^+ \end{pmatrix} \quad (32)$$

2. Compute fitness of each string by evaluating $\Pi(\Lambda^{(i)}) \forall i$
3. Rank the genetic strings where the top rank has the minimum cost function $\Pi(\Lambda^{(i)})$
4. Mate the top pairs of genetic strings to obtain 2 children (see Fig. 5), such that:

$$\Lambda^{(ci)} = \begin{pmatrix} \theta_2^{pi} \phi_1 + \theta_2^{p(i+1)} (1 - \phi_1) \\ \dots \\ p_3^{pi} \phi_{10} + p_3^{p(i+1)} (1 - \phi_{10}) \end{pmatrix}$$

where $\phi_j \in \text{rand}[0,1]$.

$$\Lambda^{(c(i+1))} = \begin{pmatrix} \theta_2^{p(i+1)} \hat{\phi}_1 + \theta_2^{pi} (1 - \hat{\phi}_1) \\ \dots \\ p_3^{p(i+1)} \hat{\phi}_{10} + p_3^{pi} (1 - \hat{\phi}_{10}) \end{pmatrix}$$

where $\hat{\phi}_j \in \text{rand}[0,1]$.

5. Remove bottom $S - P$ original strings from population. Generate $S - P - P$ new random genetic strings.
6. Repeat steps 2-5 with a new population until either one of these conditions is met:
 - G generations has been reached.
 - $\min(\Pi) \leq TOL$.

4. Numerical example

A numerical example is generated using the light model parameters in Table 1, and the optimization parameters in Table 3. An entire season was simulated with the crop model using weather data from a

Table 1
Light Model Parameters.

Symbol	Type	Units	Value	Description
N_r	scalar	none	196	Number of light rays
c	scalar	m/s	3×10^8	Speed of light
R_1	scalar	m	0.02	Solar panel thickness
n_{panel}	scalar	none	4	Number of solar panels

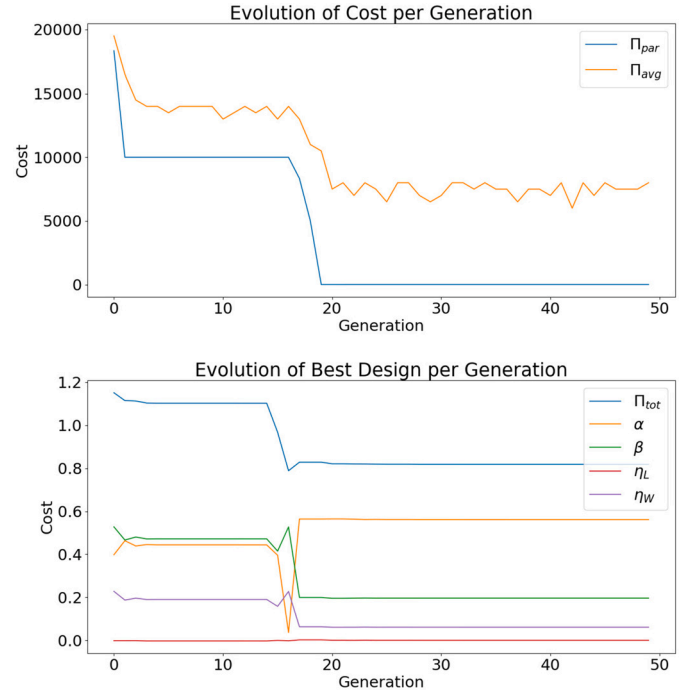


Fig. 6. Evolution of total cost Π and individual cost parameters. Top: Average cost evolution of parent and overall population. Bottom: Individual cost parameter and best design cost (excluding penalty terms) evolution.

California Irrigation Management Information System weather station [31] located in Davis, California (38.53 N, 121.77 W) from April 10, 2021 to July 19, 2021. The crop model was ran using settings in Table 2 to simulate SunnySD tomatoes for every day and hour in the aforementioned season where the altitude of the sun was above the horizon. The ground refractive index was made a variable to simulate various planting densities. The simulated agrivoltaic field has been rescaled to be of unit size to allow for smaller number of rays to be used for the light model. Lastly, the reference solar power for the agrivoltaic constraint was calculated by running the genomic optimizer to maximize solely the solar power generation.

These parameters were selected based on the values given in [18] with the only modification being to the I_{50B} term to generate a senescence more in line with expected crop behavior.

This study is presenting a framework for crop-driven agrivoltaic optimization rather than searching for the “true” optimal solution. Thus, the agrivoltaic design is optimized for 20 designs strings in the population and 50 generations of genomic optimization. The agrivoltaic design includes the altitude and azimuth angles, solar panel and ground refractive index, solar panel height, size, and shape.

The evolution of the design total cost per generation can be seen in Fig. 6 over 50 generations of optimization. The design and cost parameters associated with the optimal agrivoltaic design is tabulated in Table 4.

The “optimal” design parameters obtained through the genomic optimization scheme are used to visualize the agrivoltaic design, seen in Fig. 7.

Table 2
Crop Model Parameters.

Symbol	Units	Value	Description
Crop	none	Tomato	Crop species
Cultivar	none	SunnySD	Specific crop variety
T_{sum}	°C day	2800	Cumulative temperature requirement from sowing to maturity
HI	none	0.68	Harvest index (<i>i.e.</i> percent of harvestable biomass)
I_{50A}	°C day	520	Cumulative temperature requirement for leaf area development to intercept 50% of radiation
I_{50B}	°C day	900	Cumulative temperature till maturity to reach 50% radiation interception due to leaf senescence
I_{50maxH}	°C day	100	Maximum daily reduction in I_{50B} due to heat stress
I_{50maxW}	°C day	5	Maximum daily reduction in I_{50B} due to drought stress
T_{base}	°C	6	Base temperature for phenology development and growth
$T_{optimal}$	°C	26	Optimal temperature for biomass growth
T_{max}	°C	32	Threshold temperature to start accelerating senescence from heat stress
$T_{extreme}$	°C	45	The extreme temperature threshold when RUE becomes 0 due to heat stress
RUE	$\frac{g}{MJ \cdot m^2}$	1	Radiation use efficiency (above ground only and without respiration)
S_{CO_2}	none	0.07	Relative increase in RUE per ppm elevated CO2 above 350 ppm
S_{water}	none	2.5	Sensitivity of RUE (or harvest index) to drought stress (ARID index)
δ	none	0.66	Ratio of agrivoltaic yield to reference yield (see eq. (26))

Table 3
Genomic Optimization Parameters.

Symbol	Units	Value	Description
parents	none	6	Surviving strings for breeding
s	none	20	Designs per generation
G	none	50	Total generations
$[\theta_2^-, \theta_2^+]$	°	$[-\pi/2, \pi/2]$	Solar panel altitude angle
$[\theta_3^-, \theta_3^+]$	°	$[-\pi, \pi]$	Solar panel azimuth angle
$[\hat{n}^-, \hat{n}^+]$	none	[1,100]	Solar panel refractive index
$[h_0^-, h_0^+]$	none	[0.05,0.15]	Solar panel height
$[R_{2 \text{ or } 3}^-, R_{2 \text{ or } 3}^+]$	none	[0.0125,0.125]	Generalized radii
$[p_{1 \text{ or } 2 \text{ or } 3}^-, p_{1 \text{ or } 2 \text{ or } 3}^+]$	none	[1,20]	Geometric exponent
w_1	none	1	Weight of solar panel power in net cost
w_2	none	1	Weight of crop yield in net cost
w_3	none	1	Weight of light use efficiency in net cost
w_4	none	1	Weight of water use efficiency in net cost
P_{ref}	W	83.51	Reference solar power
Y_{ref}	$\frac{tons}{acre}$	1.7	Reference crop yield
$LU E_{ref}$	$\frac{MJ}{\frac{acre \cdot season}{tons}} / \frac{MJ}{\frac{acre \cdot season}{min}}$	0.0006	Reference light use efficiency
$WU E_{ref}$	$\frac{min}{\frac{acre \cdot season}{min}}$	0.002	Reference water use efficiency

An example of a single light pulse traveling through the medium and interacting with the surfaces is visualized using snapshots of the simulation, shown in Fig. 8. It is important to keep in mind that these light pulse simulations are done hourly for the number of days the crop is simulated. We can see that the “optimal” design places the relatively reflective ($n \approx 60$) solar panels with an altitude of 81° and azimuth angle of 290° (converting θ_3 to the azimuth angle using $\phi_{azimuth} = \theta_3 \times \frac{180}{\pi} - 90^\circ$), which results in sunlight reflecting off the panels and hitting the crops at lower solar angles.

For any simulated crop design, a variety of different outputs are available for analysis within this framework. Outputs relating to crop growth, water use and light are shown in Fig. 9. From analysis of these graphs and related data, the crop performance of an agrivoltaic crop can be compared to a reference crop. These results are discussed in the next section.

5. Discussion of results

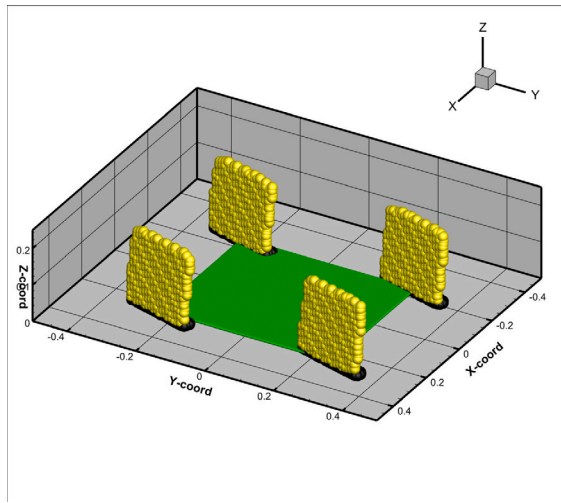
The optimized agrivoltaic design can be analyzed through the individual cost parameters that form the total cost. It can be seen that the best design has avoided violating the critical agrivoltaic constraints regarding the crop yield and solar power generation limits and incurring the large penalty terms described in Section 3. The genetic algorithm is conducting a global search within the design space and was able to obtain the presented lowest cost. Once there are designs that satisfy the soft constraints (*i.e.* negating the penalty costs), the genetic algorithm continues to reduce the cost by minimizing the individual cost parameters ($\alpha, \beta, \eta_L, \eta_W$) as much as possible. Only a limited number of designs

satisfies these agricultural constraints and reduce the cost further. The restrictions imposed by these constraints limit the design space which is the reason the cost can not be reduced beyond a certain number of generations.

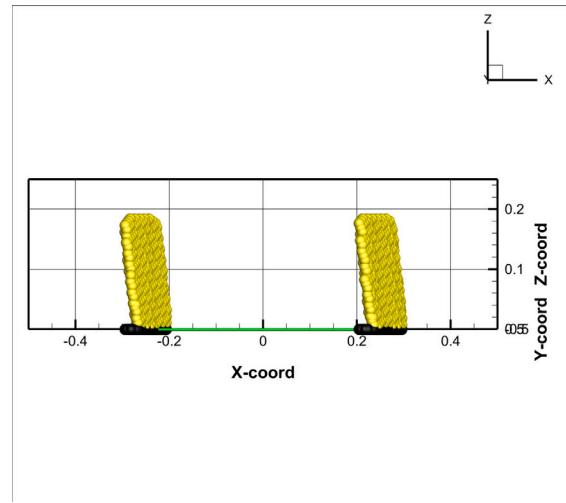
The robustness of the genetic algorithm was tested by using different seeds in the random number generator for initializing the design population and got similar optimization results. The top plot in Fig. 6 displays the parent cost for individual cost parameters which is expected to show a monotonically decreasing behavior while the average design cost is seen to be zig-zagy, which is due to random designs added to the population in each generation.

It is seen the best agrivoltaic design after 50 generations employs highly reflective near-vertical panels that reflect sunlight for crop production while still generating solar power. This is in line with the genomic optimization setup where a minimum requirement on crop production was enforced by the use of a penalty term for the crop yield cost parameter.

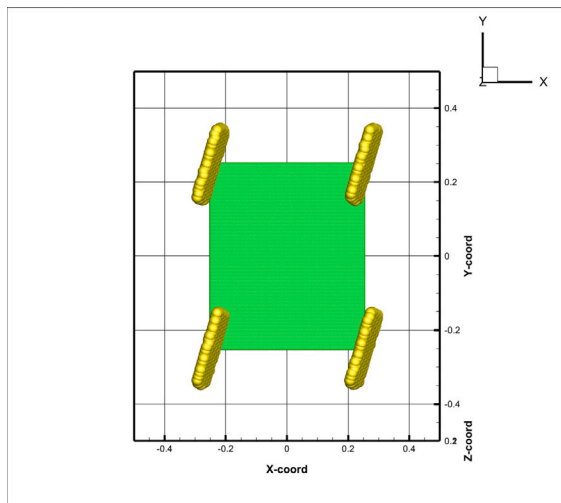
These results of nearly vertical panels are interesting as they are counter-intuitive to the theory of agrivoltaic production discussed earlier where light during the most radiation dense part of the day should be reduced to below the light saturation point. However, vertical panels match the findings of a similar design methodology [14] in Sweden which is driven more by photovoltaic performance relative to this work’s crop focused methodology. This finding is likely related to two particular limitations of this crop model: 1) a constant value is used for converting light into biomass (RUE) meaning a linear response between light and growth, and 2) the daily timestep used in the crop model does not characterize the time-sensitive responses to shading and



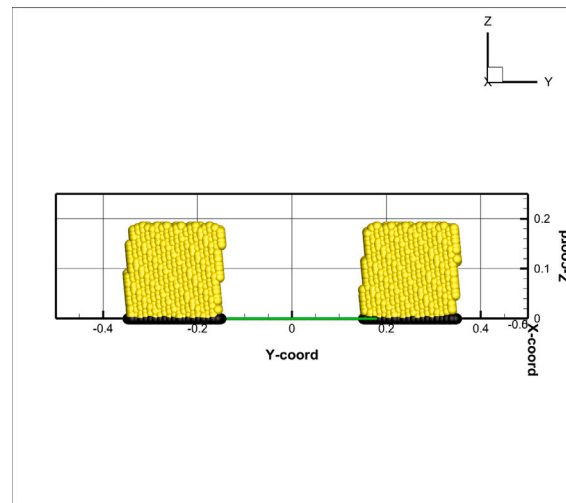
(a) Isometric view of optimized APV design.



(b) Side view of optimized APV design.



(c) Top view of optimized APV design.



(d) Front view of optimized APV design.

Fig. 7. Detailed views of optimized APV design where yellow indicates the solar panels and green represents the agricultural area.

Table 4
Optimal Agrivoltaic Design Parameters for the Numerical Example.

Π	α	β	η_L	η_W	θ_2	θ_3	\hat{n}_s
0.818	0.561	0.196	0.0	0.061	-0.154	0.344	60.64

\hat{n}_g	h_0	R_2	R_3	p_1	p_2	p_3
1.20	0.094	0.103	0.093	18.24	8.80	13.64

photosynthesis and it appears designs which maximize light when light is most dense (i.e. the afternoon) are preferred as the timing of the energy makes no difference in this implementation. This highlights the need for specific agrivoltaic crop models to be developed. Resolving these challenges are beyond the scope of this study, but the power of the framework presented allows for this modification to be made once more research is conducted into agrivoltaic crop modeling.

The cost reduction after 50 generations was determined to be 28.9% for the best design (excluding penalty terms) and 59.0% for the average design, meaning the design space was restricted to the design subspace that satisfied the agrivoltaic constraints. The crop performance as modeled was found to be 1.70 $\frac{tons}{acre}$ for the reference versus 1.43 $\frac{tons}{acre}$ for the agrivoltaic, representing an 18% loss of yield, which is less than the 34% loss acceptable in the design framework. The reference crop ET_0

was calculated to be 853 mm of water for the season compared to 751 mm of water for the agrivoltaic, representing about a 12% decrease in reference evapotranspiration.

6. Summary and extensions

Agrivoltaic systems are rapidly developing as a solution to the land competition between agriculture and solar power generation. There have been a number of modeling approaches that integrates the dynamics of the agrivoltaic system to predict crop performance and power generation. Optimization through such high fidelity models requires immense computational power. Instead, an alternative framework with a reduced order digital replica is used in tandem with a genomic optimization scheme to find optimal agrivoltaic designs. The proposed framework would help justify investment in photovoltaic arrays over agricultural settings in a way which benefits crop production using genomic multi-objective optimization to simulate the impact of photovoltaic panels on the crop environment, the subsequent crop response, and solar power generation.

Overall, this framework demonstrates potential to link light modeling with crop modeling to simulate agrivoltaic performance. Although the proposed digital replica has limitations on crop model and ray-tracing accuracy, it provides a foundational framework that utilizes a physics-driven optimization approach for agrivoltaics.

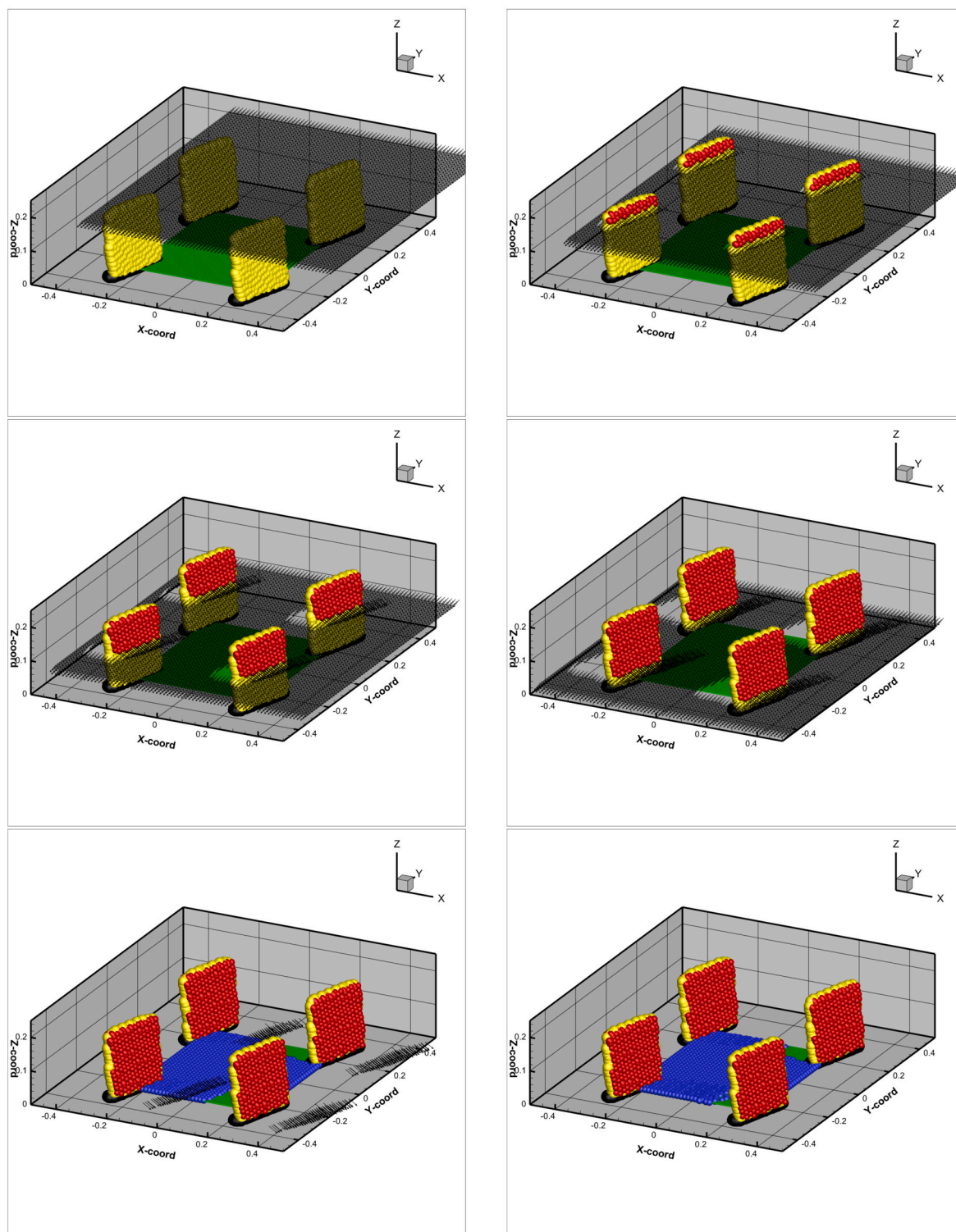


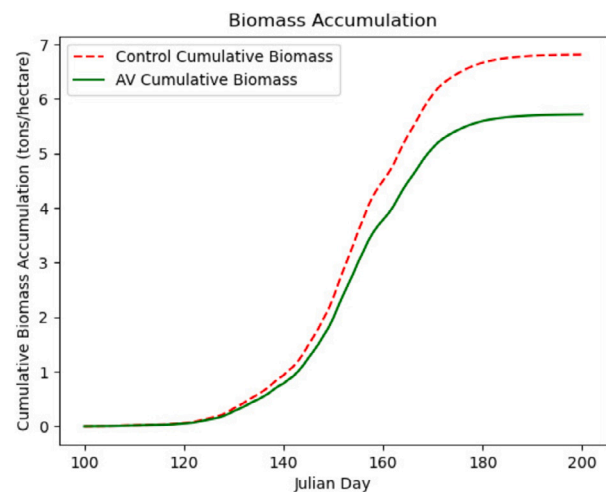
Fig. 8. Raytracing of a single light pulse. The incoming light is discretized into rays which reflect off the solar panels (shown in yellow) and hit the ground (shown in green). Solar energy is absorbed by the solar panels, at locations marked as red dots and by the ground, at locations marked as blue dots.

This model can be extended to include thermal modeling of the system, wavelength-specific raytracing, and a more advanced crop model to further increase the accuracy of the digital replica. Ultimately, a validated and refined digital replica can be used to design and test agrivoltaic configurations for a given crop, location, and desired power generation before the real-life version is built. Current work of the authors include expanding the model to include thermal modeling of the system, a more advanced crop model which captures the specific nu-

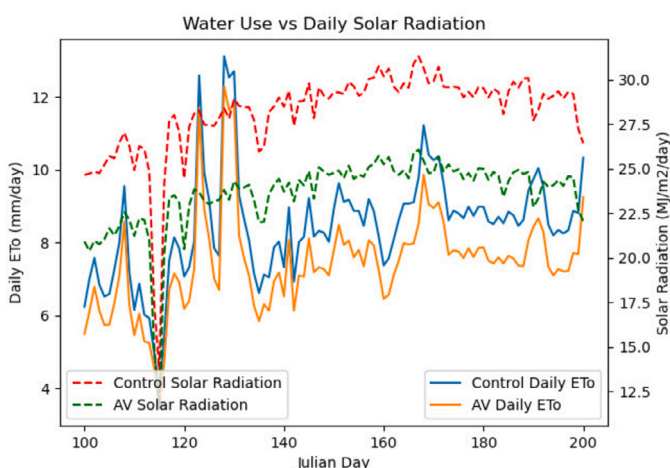
ance of agrivoltaic crop dynamics, and a water use model which looks at ET_c rather than just ET_o .

Declaration of competing interest

The authors declare that they have no known competing financial interests or personal relationships that could have appeared to influence the work reported in this paper.



(a) Cumulative biomass for control and agrivoltaic crops.



(b) Daily ETo compared with daily solar radiation.

Fig. 9. Crop model outputs.

Data availability

The authors do not have permission to share data.

Acknowledgements

This work has been partially supported by the UC Berkeley College of Engineering, and the USDA AI Institute for Next Generation Food Systems (AIFS), USDA award number 2020-67021-32855.

References

- [1] C. Dupraz, H. Marrou, G. Talbot, L. Dufour, A. Nogier, Y. Ferard, Combining solar photovoltaic panels and food crops for optimising land use: towards new agrivoltaic schemes, in: *Renewable Energy: Generation & Application*, *Renew. Energy* 36 (10) (2011) 2725–2732, <https://doi.org/10.1016/j.renene.2011.03.005>, URL <https://www.sciencedirect.com/science/article/pii/S0960148111001194>.
- [2] H. Marrou, J. Wery, L. Dufour, C. Dupraz, Productivity and radiation use efficiency of lettuces grown in the partial shade of photovoltaic panels, *Eur. J. Agron.* 44 (2013) 54–66, <https://doi.org/10.1016/j.eja.2012.08.003>, URL <https://www.sciencedirect.com/science/article/pii/S1161030112001177>.
- [3] H. Marrou, L. Guillioni, L. Dufour, C. Dupraz, J. Wery, Microclimate under agrivoltaic systems: is crop growth rate affected in the partial shade of solar panels?, *Agric. For. Meteorol.* 177 (2013) 117–132, <https://doi.org/10.1016/j.agrformet.2013.04.012>, URL <https://www.sciencedirect.com/science/article/pii/S0168192313000890>.
- [4] H. Marrou, L. Dufour, J. Wery, How does a shelter of solar panels influence water flows in a soil–crop system?, *Eur. J. Agron.* 50 (2013) 38–51, <https://doi.org/10.1016/j.eja.2013.05.004>, URL <https://www.sciencedirect.com/science/article/pii/S1161030113000683>.
- [5] S. Schindele, M. Trommsdorff, A. Schlaak, T. Obergfell, G. Bopp, C. Reise, C. Braun, A. Weselek, A. Bauerle, P. Högy, A. Goetzberger, E. Weber, Implementation of agrophotovoltaics: techno-economic analysis of the price-performance ratio and its policy implications, *Appl. Energy* 265 (2020) 114737, <https://doi.org/10.1016/j.apenergy.2020.114737>, URL <https://www.sciencedirect.com/science/article/pii/S030626192030249X>.
- [6] M.A.A. Mamun, P. Dargusch, D. Wadley, N.A. Zulkarnain, A.A. Aziz, A review of research on agrivoltaic systems, *Renew. Sustain. Energy Rev.* 161 (2022) 112351, <https://doi.org/10.1016/j.rser.2022.112351>, URL <https://www.sciencedirect.com/science/article/pii/S1364032122002635>.
- [7] M. Kadowaki, A. Yano, F. Ishizu, T. Tanaka, S. Noda, Effects of greenhouse photovoltaic array shading on welsh onion growth, *Biosyst. Eng.* 111 (3) (2012) 290–297, <https://doi.org/10.1016/j.biosystemseng.2011.12.006>, URL <https://www.sciencedirect.com/science/article/pii/S1537511011002273>.
- [8] R. Ureña-Sánchez, Á.J. Callejón-Ferre, J. Pérez-Alonso, Á. Carreño-Ortega, Greenhouse tomato production with electricity generation by roof-mounted flexible solar panels, *Sci. Agric.* 69 (4) (2012) 233–239.
- [9] Y. Elamri, B. Cheviron, J.-M. Lopez, C. Dejean, G. Belaud, Water budget and crop modelling for agrivoltaic systems: application to irrigated lettuces, *Agric. Water Manag.* 208 (2018) 440–453, <https://doi.org/10.1016/j.agwat.2018.07.001>, URL <https://www.sciencedirect.com/science/article/pii/S0378377418309545>.
- [10] E. Hassanpour Adeh, J.S. Selker, C.W. Higgins, Remarkable agrivoltaic influence on soil moisture, micrometeorology and water-use efficiency, *PLoS ONE* 13 (11) (2018) e0203256.
- [11] S. Amaducci, X. Yin, M. Colauzzi, Agrivoltaic systems to optimise land use for electric energy production, *Appl. Energy* 220 (2018) 545–561, <https://doi.org/10.1016/j.apenergy.2018.03.081>, URL <https://www.sciencedirect.com/science/article/pii/S0306261918304197>.
- [12] A. Yamada, S. Ogata, Potential evaluation of agrivoltaic case of Kyoto prefecture Japan, in: *AIP Conference Proceedings*, vol. 2361, AIP Publishing LLC, 2021, p. 020003.
- [13] M.H. Riaz, H. Imran, R. Younas, N.Z. Butt, The optimization of vertical bifacial photovoltaic farms for efficient agrivoltaic systems, *Sol. Energy* 230 (2021) 1004–1012, <https://doi.org/10.1016/j.solener.2021.10.051>, URL <https://www.sciencedirect.com/science/article/pii/S0038092X21009087>.
- [14] P.E. Campana, B. Stridh, S. Amaducci, M. Colauzzi, Optimisation of vertically mounted agrivoltaic systems, *J. Clean. Prod.* 325 (2021) 129091.
- [15] T. Zohdi, A digital-twin and machine-learning framework for the design of multiobjective agrophotovoltaic solar farms, *Comput. Mech.* 68 (2) (2021) 357–370.
- [16] R. Isied, E. Mengi, T. Zohdi, A digital-twin framework for genomic-based optimization of an agrophotovoltaic greenhouse system, *Proc. R. Soc. A, Math. Phys. Eng. Sci.* 478 (2267) (2022), <https://doi.org/10.1098/rspa.2022.0414>.
- [17] B. Stafford, *pysolar* (0.9), <https://doi.org/10.5281/zenodo.5518074>, 2020.
- [18] C. Zhao, B. Liu, L. Xiao, G. Hoogenboom, K.J. Boote, B.T. Kassie, W. Pavan, V. Shelia, K.S. Kim, I.M. Hernandez-Ochoa, D. Wallach, C.H. Porter, C.O. Stockle, Y. Zhu, S. Asseng, A simple crop model, *Eur. J. Agron.* 104 (2019) 97–106, <https://doi.org/10.1016/j.eja.2019.01.009>, URL <https://www.sciencedirect.com/science/article/pii/S1161030118304234>.
- [19] S. von Caemmerer, G. Farquhar, J. Berry, *Biochemical Model of C3 Photosynthesis*, Springer Netherlands, Dordrecht, 2009, pp. 209–230, Ch. 9.
- [20] A. Senevirathna, C. Stirling, V. Rodrigo, Acclimation of photosynthesis and growth of banana (*Musa sp.*) to natural shade in the humid tropics, *Exp. Agric.* 44 (3) (2008) 301–312.
- [21] A. Senevirathna, C. Stirling, V. Rodrigo, Growth, photosynthetic performance and shade adaptation of rubber (*hevea brasiliensis*) grown in natural shade, *Tree Physiol.* 23 (10) (2003) 705–712.
- [22] P. Siles, O. Bustamante, E. Valdivia, J. Burkhardt, C. Staver, Photosynthetic performance of banana ('gros michel', AAA) under a natural shade gradient, in: *VII International Symposium on Banana: ISHS-ProMusa Symposium on Bananas and Plantains: Towards Sustainable Global Production* 986, 2011, pp. 71–77.
- [23] N.F. Othman, M.E. Yaacob, A.S. Mat Su, J.N. Jaafar, H. Hizam, M.F. Shahidan, A.H. Jamaluddin, G. Chen, A. Jalaludin, Modeling of stochastic temperature and heat stress directly underneath agrivoltaic conditions with orthosiphon stamineus crop cultivation, *Agronomy* 10 (10) (2020), <https://doi.org/10.3390/agronomy10101472>, URL <https://www.mdpi.com/2073-4395/10/10/1472>.
- [24] J.L. Monteith, Evaporation and Environment, *Symposia of the Society for Experimental Biology*, vol. 19, Cambridge University Press (CUP), Cambridge, 1965, pp. 205–234.
- [25] A. Weselek, A. Bauerle, J. Hartung, S. Zikeli, I. Lewandowski, P. Högy, Agrivoltaic system impacts on microclimate and yield of different crops within an organic crop rotation in a temperate climate, *Agron. Sustain. Dev.* 41 (5) (2021) 1–15.
- [26] M. Elborg, Reducing land competition for agriculture and photovoltaic energy generation—a comparison of two agro-photovoltaic plants in Japan, in: *International Conference on Sustainable and Renewable Energy Development and Design, SREDD2017*, vol. 3, 2017, p. 5.
- [27] F. Letternmeier, E. Gimbel, A. Schlaak, S. Schindele, T. Keinath, A. Steinhuser, M. Trommsdorff, C. Lindenmeyer, I.G. Mair, A. Lachhammer, F. Hilber, D.-I.F.M. Balz, P.D.M. Schlaich, M. Bohn, D.G. Weinrebe, M.D.F. Eisel, M.G. Heintze, T. Huttmeier,

- J. Mack, J. Mayer, J. Bruckner, J. Lenck, D.-I.F.J. Wagner, F. Kameoka, a.P.D.P. Hody, L. Pataczek, D.S. Zikeli, Agri-photovoltaic systems – Requirements for primary agricultural use English translation of DIN SPEC 91434:2021-05, Standard, Deutsches Institut für Normung, Berlin, Germany, May 2021.
- [28] M. D. of Energy Resources, Energy Resources, Solar Massachusetts Renewable Target (SMART) Program regulation 225 CMR 20.00, Program regulations, Massachusetts Department of Energy Resources, Massachusetts, United States, 2021, URL <https://www.mass.gov/doc/225-cmr-2000-final-071020-clean/download>.
- [29] B. Valle, T. Simonneau, F. Sourd, P. Pechier, P. Hamard, T. Frisson, M. Ryckewaert, A. Christophe, Increasing the total productivity of a land by combining mobile photovoltaic panels and food crops, *Appl. Energy* 206 (2017) 1495–1507, <https://doi.org/10.1016/j.apenergy.2017.09.113>, URL <https://www.sciencedirect.com/science/article/pii/S0306261917313971>.
- [30] R. Mead, R.W. Willey, The concept of a 'land equivalent ratio' and advantages in yields from intercropping, *Exp. Agric.* 16 (3) (1980) 217–228, <https://doi.org/10.1017/S0014479700010978>.
- [31] S. of California, California irrigation management information system, <https://cimis.water.ca.gov/Default.aspx>, 2022.